A Model Predictive Control based Peak Shaving Application for a Grid Connected Household with Photovoltaic and Battery Storage

Deepranjan Dongol, Thomas Feldmann and Elmar Bollin
Institute of Energy Systems Technology (INES), Offenburg University of Applied Sciences, Am Güterbahnhof 1a, 77652, Offenburg, Baden-Württemberg, Germany

Keywords: Mixed Integer Quadratic Programming, Peak Shaving, Model Predictive Control.

Abstract: The increase in households with grid connected Photovoltaic (PV) battery system poses challenge for the grid due to high PV feed-in as a result of mismatch in energy production and load demand. The purpose of this paper is to show how a Model Predictive Control (MPC) strategy could be applied to an existing grid connected household with PV battery system such that the use of battery is maximized and at the same time peaks in PV energy and load demand are reduced. The benefits of this strategy are to allow increase in PV hosting capacity and load hosting capacity of the grid without the need for external signals from the grid operator. The paper includes the optimal control problem formulation to achieve the peak shaving goals along with the experiment set up and preliminary experiment results. The goals of the experiment were to verify the hardware and software interface to implement the MPC and as well to verify the ability of the MPC to deal with the weather forecast deviation. A prediction correction has also been introduced for a short time horizon of one hour within this MPC strategy to estimate the PV output power behavior.

1 INTRODUCTION

In Germany, households with grid-connected photovoltaic (PV) systems have increased significantly over the years as a result of favorable feed-in tariff and subsidy policy. Households with PV installations are typically under 10 kWp and comprise about 15% of the total installed PV power in Germany (Wirth and Schneider, 2013). A low-voltage (LV) distribution grid with a pool of such household prosumers can be considered to be a distributed renewable energy source. Apart from influencing the electricity price in the market and the renewable energy policies, such a situation poses a challenge to the technical aspect of the distribution grid. This is particularly a problem for the residential network where the mismatch in power generation and load demand result in a high PV feed-in.

Distribution lines are designed to deliver power from distribution stations to the consumers. The power-flow reversal resulting from the integration of prosumers who feed energy into the grid causes the voltage to rise at the coupling point. The VDE AR-N 4105 grid standard in Germany allows only a maximum 3% increase in the nominal voltage caused by PV penetration (Spring and Witzmann, 2014). A case of an overvoltage problem in Germany due to high PV feed-in into the distribution grid has been presented in (Stetz et al., 2013). In order to keep the voltage within the permissible limit, the regulation in Germany suggests the feed-in to be restricted to 70% of the installed peak PV power capacity (Spring and Witzmann, 2014). But this often leads to power curtailments of useful PV power (Weniger et al., 2014; Castillo-Cagigal et al., 2011). In a conventional PV battery operation, the controller does not foresee PV energy production or load demand. The controller knows the State of Charge (SOC) of the battery only for the present time. As such, the battery is often completely charged before the peak PV energy production period, which results in a high PV feed-in and therefore cannot mitigate the voltage rise problem (Castillo-Cagigal et al., 2011). In such a situation, the feed-in limit can only be achieved by active power curtailment (Tonkoski et al., 2011) or reactive power control (Turitsyn et al., 2010; Weckx et al., 2014).

The use of a battery allows the household prosumers to achieve Demand-Side Management (DSM) for themselves at a local level, independent of the grid operator. DSM is a concept to improve

Dongol, D., Feldmann, T. and Bollin, E.
A Model Predictive Control based Peak Shaving Application for a Grid Connected Household with Photovoltaic and Battery Storage.
DOI: 10.5220/0006685300540063
In *Proceedings of the 7th International Conference on Smart Cities and Green ICT Systems (SMARTGREENS 2018)*, pages 54-63
ISBN: 978-989-758-292-9

the energy consumption behavior of the consumers, primarily for economic operation and in order to maximize the consumption of renewable energy by balancing the mismatch in energy production and load demand. Real-Time Price (RTP), Time of Use (TOU) and Critical Peak Pricing (CPP) are seen as key DSM programs to reduce the peak load demand in the grid (Herter, 2007; Palensky, 2011; Yang et al., 2014). In recent years , the concepts of automated home systems have also emerged as a part of Demand-Response (DR) strategies for the optimal scheduling of electrical appliances in order to respond to the price-driven DSM programs (Costanzo et al., 2011; Di Giorgio and Liberati, 2014; Moraiset et al., 2014).

In this work, the optimal control problem has been formulated for a single grid electricity price and single feed-in tariff scenarios, which is very likely to remain a standard for a long time. Therefore, the optimal control problem presented in this paper is not dictated by price but rather by the predicted PV output power and the load-demand profile. From an economic operation point of view and considering the cost benefits by using the battery from (Riffonneau et al., 2011), it is justifiable to assume that maximizing the use of the battery is cost-effective for the prosumer. In order to implement the optimal control problem and to deal with the forecast uncertainties, the MPC approach has gained increased attention in recent years. Its ability to update itself based on the measurement of the system and to re-optimize the power flow at each control-time interval – which is also known as the receding horizon approach – has been presented in (Wu et al., 2015; Parisio et al., 2014). Most of the optimal control problems are developed with an understanding that the receding horizon feature of the MPC can handle the forecast uncertainties, as mentioned by (Arnold and Andersson, 2011). Therefore, the MPC approach can be considered to be the state of the art for the implementation of optimal control problems. In this paper, the proposed MPC is applied to the existing system in the laboratory for preliminary tests and it is assumed that the size of the battery is enough to shave the peak PV energy to avoid active power curtailment or exceed the feed-in limit.

2 METHODOLOGY

The schematic of a household with a grid-connected PV battery system is shown in Figure 1. At any time interval, P_{v_i} is the output power of the installed PV, P_{L_i} is the load demand, P_{bc_i} is the battery charging power, P_{bdc_i} is the battery discharging power, P_{gf_i} is the power fed into the grid, and P_{gc_i} is the grid power consumption. The sign convention of respective variables for the optimal power problem is consistent throughout this paper, as shown in Figure 1. The grid is used as a virtual storage to take in any surplus energy from the PV and as a backup when the load demand exceeds the battery converter size or when the stored battery energy is not sufficient. The power flow within the system satisfies the power-flow balance which can be expressed as

$$P_{v_i} - P_{L_i} = P_{gf_i} + P_{bc_i} + P_{bdc_i} + P_{gc_i} \quad (1)$$

2.1 Battery Storage Dynamics

A linear power-flow model was used to represent the dynamic behavior of the battery and to thus measure the battery SOC. The battery model is discretized as

$$x_{i+1} = x_i + \eta_{ch} \cdot P_{bc_i} \cdot \Delta t + (1/\eta_{dch}) \cdot P_{bdc_i} \cdot \Delta t - L_{batt,loss} \cdot \Delta t \quad (2)$$

The battery energy for the time interval i+1 is calculated as the sum of battery energy x_i and the

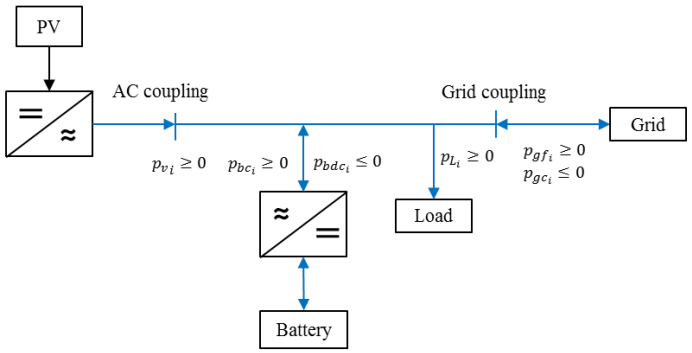

Figure 1: Schematic of the grid-connected PV battery system.

battery power flow P_{bc_i} or P_{bdc_i} at time interval i. Δt is the duration of the time interval. In this paper, the duration of the time interval for the optimal control problem is defined as 10 minutes. The efficiency of the charging and discharging processes is defined by variables η_{ch} and η_{dch} respectively. The battery converter components consume power from the battery and are represented by $L_{batt,loss}$ which was considered to be constant throughout the battery operation. For the optimal control problem, if E_{batt} is the nominal capacity of the battery, the battery SOC's percentage is expressed as

$$SOC_{i+1} = (x_{i+1}/E_{batt}) \times 100 \quad (3)$$

In order to avoid the concurrent charging and discharging of the battery, a logical condition of $P_{bc_i} \cdot P_{bdc_i} = 0$ arises. It is represented as a linear inequality by using binary variables as follows:

$$P_{bc_i} = \begin{cases} 0 \le P_{bc_i} \le P_{Max} & \text{, if } \delta_{bc}=1 \\ 0 & \text{, otherwise} \end{cases} \quad (4)$$

$$P_{bdc_i} = \begin{cases} -P_{Max} \le P_{bdc_i} \le 0 & \text{, if } \delta_{bdc}=1 \\ 0 & \text{, otherwise} \end{cases} \quad (5)$$

For the optimal control problem, Eq. 4 and Eq. 5 can be reformulated as

$$0 \le P_{bc_i} \le P_{Max} \cdot \delta_{bc_i} \quad (6)$$

$$-P_{Max} \cdot \delta_{bdc_i} \le P_{bdc_i} \le 0 \quad (7)$$

Here, P_{Max} is the maximum rated power of the battery converter. Eq. 4 and Eq. 5 indicate that battery charging or discharging only occur when the corresponding binary variables δ_{bc} or δ_{bdc} are 1 respectively. Therefore, the concurrent charging and the discharging of the battery is avoided by defining a binary inequality constraint as

$$\delta_{bc_i} + \delta_{bdc_i} \le 1 \quad (8)$$

Eq. 8 shows that either δ_{bc_i} or δ_{bdc_i} can have the value of 1. Battery operation is restricted by its rated capacity to store the maximum level of energy as well as the Depth of Discharge (DOD) provided by the battery manufacturer for the recommended level of discharge. This constraint on the battery SOC can be expressed as

$$x_{Min} \le x_{i+1} \le x_{Max} \quad (9)$$

$$x_{Min} = (1 - DOD) \cdot x_{Max} \quad (10)$$

Here, $x_{Max} = E_{batt}$ is the rated capacity of the battery.

2.2 Interaction with the Grid

As in the case of the battery, binary variables are introduced in order to avoid the concurrent grid feed-in and grid power consumption to reformulate the logic constraint of $P_{gf_i} \cdot P_{gc_i} = 0$ as

$$P_{gf_i} = \begin{cases} 0 \le P_{gf_i} \le P_{v_i} & \text{, if } \delta_{gf} = 1 \\ 0 & \text{, otherwise} \end{cases} \quad (11)$$

$$P_{gc_i} = \begin{cases} -P_{g_{Max}} \le P_{gc_i} \le 0 & \text{, if } \delta_{gc}=1 \\ 0 & \text{, otherwise} \end{cases} \quad (12)$$

$$\delta_{gf_i} + \delta_{gc_i} \le 1 \quad (13)$$

For the optimal control problem, Eq. 11 and Eq. 12 can be expressed as

$$0 \le P_{gf_i} \le P_{v_i} \cdot \delta_{gf_i} \quad (14)$$

$$-P_{g_{Max}} \cdot \delta_{gc_i} \le P_{gc_i} \le 0 \quad (15)$$

In Eq. 14, the maximum grid feed-in is restricted by the PV output power P_{v_i}. Likewise, in Eq. 15, the maximum grid consumption $P_{g_{Max}}$ is defined as the maximum possible grid consumption for the system. $P_{g_{Max}}$ is set to a very high fixed value compared to the peak-power demand so that the required grid consumption always takes place within it.
This has been done to make the solution feasibleIt doesn't affect the optimal solution due to the power-flow balance constraint of Eq. 1. The concurrent grid feed-in and grid consumption is avoided with Eq. 13. Furthermore, the battery is not allowed to interact with the grid as the optimal control problem is designed for a maximum usage of self-produced electricity by using the battery for a single grid electricity price and a single feed-in tariff scenario. Therefore, the charging of the battery from and its discharging to the grid is forbidden, which leads to the logical conditions $P_{bc_i} \cdot P_{gc_i} = 0$ and $P_{bdc_i} \cdot P_{gf_i} = 0$, which are then expressed as

$$\delta_{gf_i} + \delta_{bdc_i} \le 1 \quad (16)$$

$$\delta_{gc_i} + \delta_{bc_i} \le 1 \quad (17)$$

2.3 Optimal Control Problem

The PV power output is defined in a N×1 vector as $\underline{P_v} = [p_{v_i} \quad \cdots \quad p_{v_{i+N-1}}]^T$ over the prediction horizon of 24 hours, where N is the number of time steps. Similarly, the load demand over the prediction horizon is defined in a N×1 vector as $\underline{P_L}$=

$[p_{L_i} \cdots p_{L_{i+N-1}}]^T$.The difference between the predicted PV output power and the predicted load demand for each time interval i over the prediction horizon is defined in a new N×1vector as $\underline{P_{in}}=\underline{P_v}-\underline{P_L}=[p_{in_i} \cdots p_{in_{i+N-1}}]^T$.

The vector $\underline{P_{in}}$ provides the reference for the battery operation over the prediction horizon. For a prediction horizon of 24 hours, the number of time intervals N with a time interval of 10 minutes is obtained as, $N=(24\times60)/10=144$.

The objective of the optimal control problem formulation is to find the optimal values for P_{bc_i} and P_{bdc_i} so as to reduce the PV feed-in to the grid as well as grid power consumption. As the problem has reference and target variables along with binary constraints, the optimal control problem has been formulated as a Mixed Integer Quadratic (MIQP) problem as

$$\min_u \sum_i^{i+N-1} \frac{1}{2} u_i^T R u_i \quad (18)$$

Subject to: Eq. 1 - 3, Eq. 6 - 9 and Eq. 13 - 17

Where,

$$u_i=\begin{bmatrix} P_{in_i}-P_{bc_i} \\ P_{in_i}-P_{bdc_i} \\ P_{gc_i} \end{bmatrix} \text{ and } R=\begin{bmatrix} 100 & 0 & 0 \\ 0 & 100 & 0 \\ 0 & 0 & 2000 \end{bmatrix}.$$

The quadratic penalty on $P_{gc_i}^2$ ensures that the grid power consumption is very low, with peaks reduced. The penalties on the squared differences $(P_{in_i}-P_{bc_i})^2$ and $(P_{in_i}-P_{bdc_i})^2$ ensure that the battery power flow reaches as close as possible to the reference $\underline{P_{in}}$, thereby prioritizing the peaks. Due to the power flow balance in Eq. 1, the value of P_{gf_i} is obtained automatically from the optimal solution. The weighting matrix R has been defined by the user to be suitable for this process.

2.4 PV Power-Prediction Update

To correct the PV prediction, a linear interpolation for the next 1 hour was applied based on the PV power measurement at an interval. This correction procedure is also shown in Figure 2. The initially predicted PV data from the day-ahead forecast is available as $\underline{P_v}=[p_{v_i} \cdots p_{v_{i+N-1}}]$ with a time resolution of 10 minutes. So for a given time intervali, if $P_{v_{meas_i}}$ is the measured PV output power and $P_{v_{i+6}}$ the initially predicted value at an hour-ahead interval i+6, the formula for the linear interpolation between two points is given by

$$\underline{P_c}=P_{v_{meas_i}}+(\hat{i}-i)\cdot((P_{v_{i+6}}-P_{v_{meas_i}})/((i+6)-i)) \quad (19)$$

Where, $\hat{i} \in [i+1, i+5]$

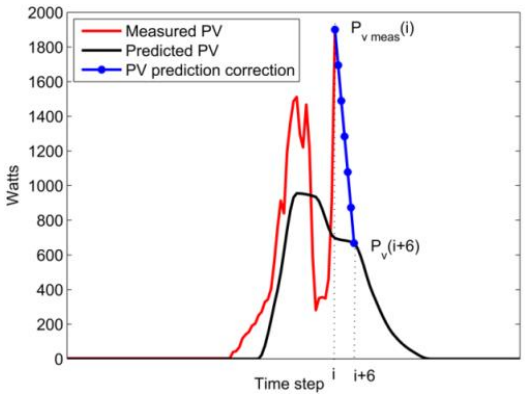

Figure 2: PV prediction-correction method by using linear interpolation.

3 MPC STRATEGY

The proposed MPC implementation scheme for the experiment is shown in Figure 3. The weather forecast data are collected every 24 hours from the weather service provider. The global solar insolation (G_h), the ambient temperature (T_{amb}) and relative humidity data (r_h) are obtained as weather forecast data for every hour. The predicted PV output power with the prediction model described in (Schmelas et al., 2015) is then interpolated for every 10 minutes by using Piecewise Cubic Hermite Data interpolation. The load profile prediction is collected from the database. The predicted PV data $\underline{P_v}$, along with the load profile $\underline{P_L}$ and the initialized battery SOC $\hat{x}_i$ from the measurement is then provided so as to solve the optimal control problem, which results in a sequence of optimal control values: $u_i, u_{i+1}, u_{i+2}, \ldots u_{i+N-1}$. Only the first optimal value u_i for the first control interval i is provided as a local command to the battery converter in order to control battery power flow. Towards the end of each control time interval, the measured PV output power is used to correct the PV prediction which then updates the predicted PV output-power profile as $\widehat{\underline{P_v}}$. The load profile is automatically updated within the system. Load demand was considered to be perfect and virtual as there was no real load available due to the limitations in the laboratory infrastructure. So the

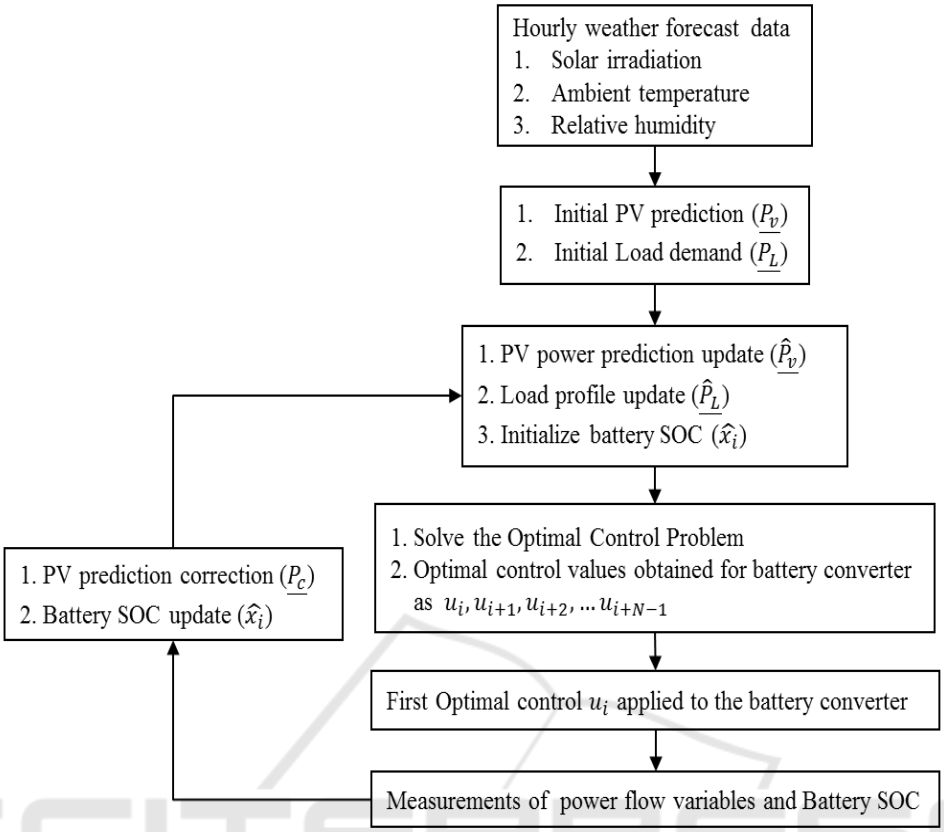

Figure 3: Proposed MPC approach used for the experiment.

optimal discharging of the battery was considered to fulfill the load-demand case. There is also no real grid power consumption, but only the reduction in the load demand .The expected grid power consumption is calculated from the power-flow balance in Eq. 1. The measured battery SOC $\hat{x}_i$ is used again in order to update and initialize before another optimal control problem is solved. This process is then repeated online.

3.1 Experiment Setup Description

The schematic of the MPC implemented in the laboratory system is shown in Figure 4. The experiment setup consisted of an installed 2.1 kWp PV system. The PV installation was AC-coupled with the experimental micro-grid by using a 2.2 kWp PV inverter. A 1.8 kWp battery converter connected the battery with this micro-grid. It was used to control battery power flow based on the command given to it. A deep-discharge 3 kWh lithium-ion battery was used for the experiment. This micro-grid was also coupled with the main grid. As mentioned before, the load demand is virtual and has only been shown for the sake of representation. It should be noted that the measurements $P_{v_{meas}}$, P_{bc}, P_{bdc} and x were measured directly from the real system. However, since P_L is virtual, P_{gc} was derived from the calculation. The schematic of the communication between the hardware and the software interface used in this experiment is shown in Figure 5. The weather forecast data and the load-demand profile were read from a MS-SQL server database. The weather forecast data were updated every 24 hours. These data were loaded into MATLAB by using SQL commands. The optimal control problem was solved in MATLAB using CPLEX solver. The optimal value of battery power flow for the corresponding control time interval was transferred from MATLAB into the SQL server database by using SQL commands. LABVIEW was used as an interface between the SQL server database and the CX2040 Beckhoff Programmable Logic Controller (PLC) by using the OPC UA communication protocol to visualize the process. Otherwise, the PLC could read directly from the MS-SQL server database as well. The PLC then sets the optimal battery power-flow value in the battery

Table 1: System specification in the experiment setup.

System description	Specification
Installed PV array capacity	2.1 kWp
Installed PV inverter capacity	2.2 kWp
Nominal battery capacity (E_{batt})	3 kWh
SOC_{Max}	100 %
SOC_{Min}	15 %
Battery converter size (P_{Max})	1.8 kWp
Battery charging efficiency (η_{ch})	85 %
Battery discharging efficiency (η_{dch})	95 %

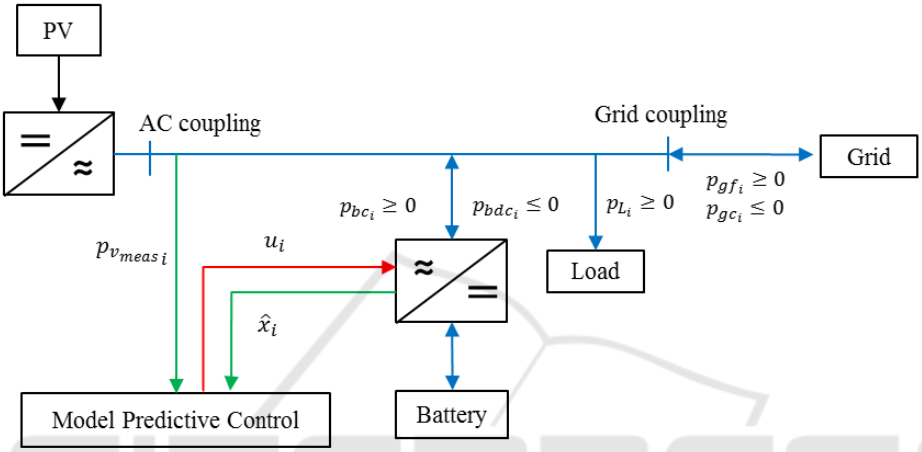

Figure 4: Schematic of the experiment setup using the proposed MPC strategy.

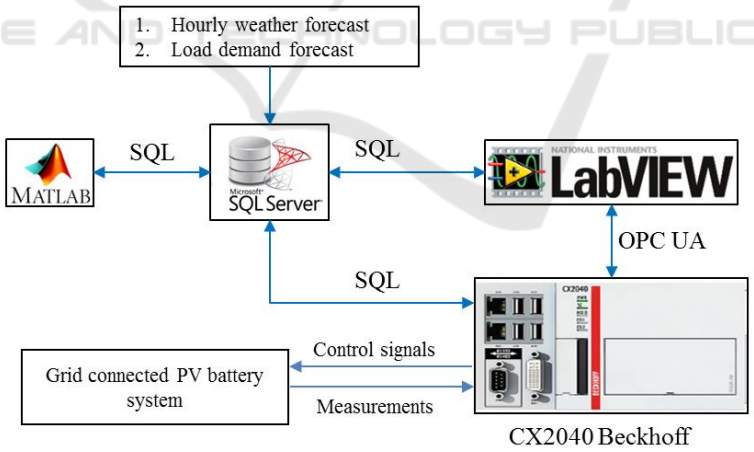

Figure 5: Schematic of communication between MPC and PV battery system.

converter, as well as taking relevant measurements from the system. The PLC also writes the measured data into the SQL server database which is then loaded into the MATLAB. This approach was chosen since the MATLAB 2014a version does not support the OPC UA protocol.

The system parameters used for the experiment are shown in Table 1.

3.2 Preliminary Experiment Results

In order to test the effectiveness of the proposed MPC strategy, the preliminary experiment was conducted during the consecutive cloudy days of October 11 and 12 in 2016. These two days were chosen based on weather forecast data. The results presented in this paper are mean values of the measurements over the control interval. The initially predicted and the measured PV output power at the end of the experiment is shown in Figure 6, with huge deviations as expected. The experiment results from the proposed MPC strategy are shown in Figure 7 and Figure 8. They are presented with a time resolution of 10 minutes. The results show that the PV prediction-correction method is able to estimate the behavior of PV output power. Its random peaks due to clouds have been detected. This, along with the receding horizon feature of the MPC, is able to optimally control battery power flow, effectively dealing with the deviations in the PV prediction errors. The battery charging is optimally controlled when peaks in PV power production occur. Furthermore, the optimal discharge of the battery reduced the peak-load demand during the evening and the following morning, owing to the receding horizon feature of the MPC. The loss in the battery due to self-consumption from the power electronics of the converter was measured to be around 10 watts. Due to the optimal discharge of the battery, the Load Demand Reduction (LDR) is high for the higher values of load demand, as shown in Figure 9. The LDR was calculated as

$$\text{LDR}\ (\%) = \left(P_{dc_i} / P_{L_i} \right) \times 100 \qquad (20)$$

The resulting SOC profile for this experiment is shown in Figure 10. Since a linear power-flow model of the battery was used to predict the battery SOC, it is quite understandable that the non-linear dynamics of the battery were not captured well. As can be seen in Figure 10, there was a sudden increase in the SOC from 17 to 18 hours. If a very complex non-linear model of the battery is to be used, the entire problem formulation becomes non-linear and non-convex and hence, the optimal control problem needs to be reformulated as a Dynamic Programming (DP) problem (Riffonneau et al., 2011). However, in our case, the continuous update of the SOC restricted battery operation within its defined SOC boundary conditions and allowed for an optimal use of the battery. Therefore, the linear power-flow model is still effective to estimate the behavior of the battery.

But there is a limitation in this experiment with respect to the time resolution of the MPC. When the change in PV power production with respect to time ($\Delta P_v / \Delta t$) was faster than the MPC time resolution of 10 minutes, the controller was not able to take any control action. Figure 10 shows that due to this, during the first charging period after 11 and 13 hours, the battery charging power was at times more than the surplus PV output power. This situation can also be seen after 17 and 18 hours as well as after 34 and 36 hours. So during this time, grid power was consumed in order to charge the battery, which was an error. There was also a PV feed-in to the grid after 16, 38 and 39 hours due to this time-resolution limitation. The time required for one complete MPC loop in an interval for this experiment was around 10 seconds from obtaining the predicted and measured data to solving the optimal control problem and finally sending the control signal to the battery converter. It should be noted that increasing the time resolution of the optimal control problem also reduces the speed of solving it. And with a further increase in time resolution, the problem might get beyond the solver's capability. This was the reason to consider 10 minutes as a benchmark time resolution for this experiment – as the goal was only to verify the behavior of the MPC, which was as expected. Since this was just a preliminary test, the MPC performance does provide a motivation to upgrade the MPC strategy for real-time operation. The use of a two-level control by using optimal scheduling and an MPC loop (as presented in (Petrollese et al., 2016) provides a scope of upgrading the MPC approach used in this experiment for real-time application. Despite the fact that the experiment results were not as ideal as expected, the behavior of the proposed MPC approach in dealing with the weather forecast uncertainties (as for PV energy prediction) and the disturbance (as with the battery SOC) were well-captured.

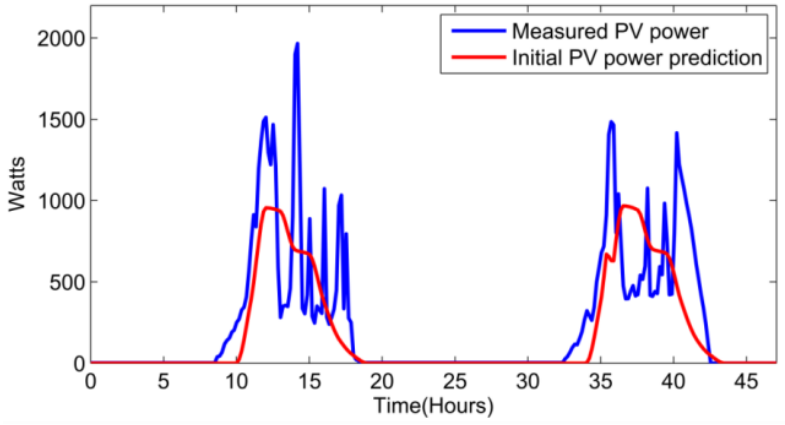

Figure 6: Predicted and measured PV power output.

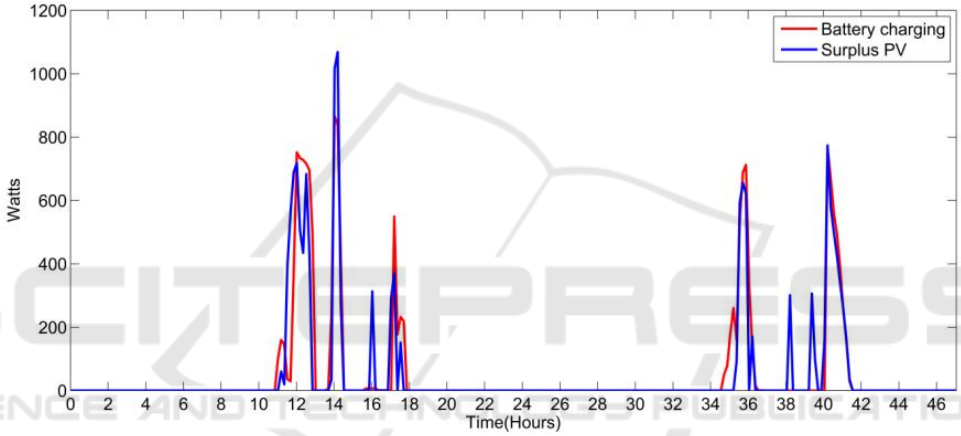

Figure 7: Experiment results for the optimal charging of the battery.

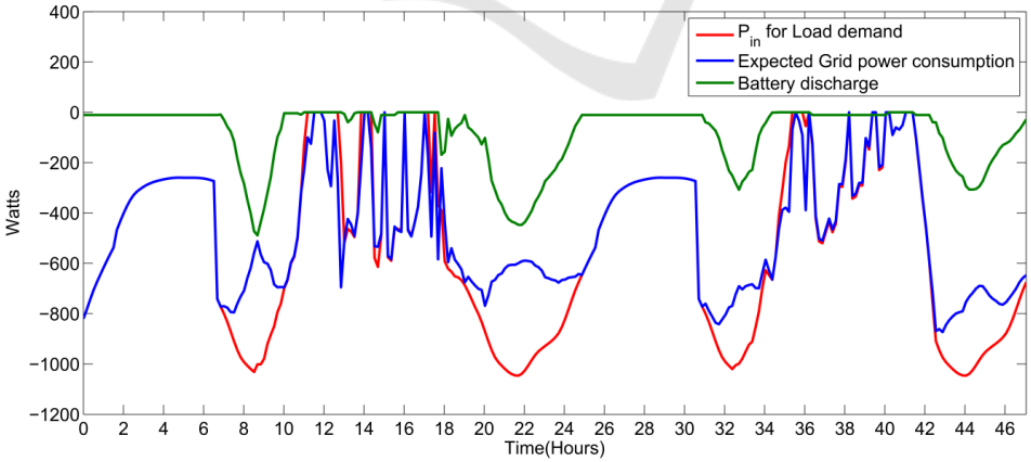

Figure 8: Experiment results for the optimal discharge of the battery.

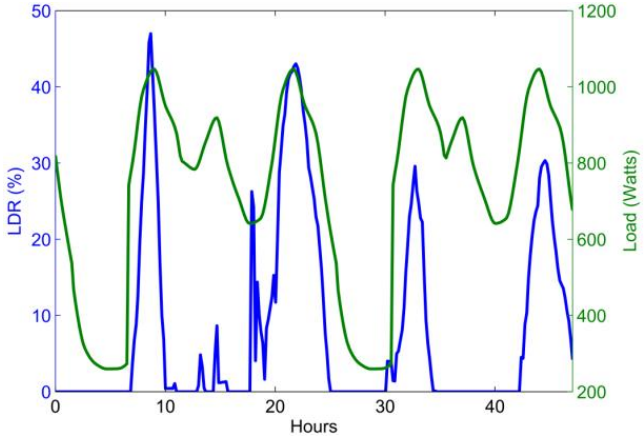

Figure 9: Reduction in Load demand from the experiment.

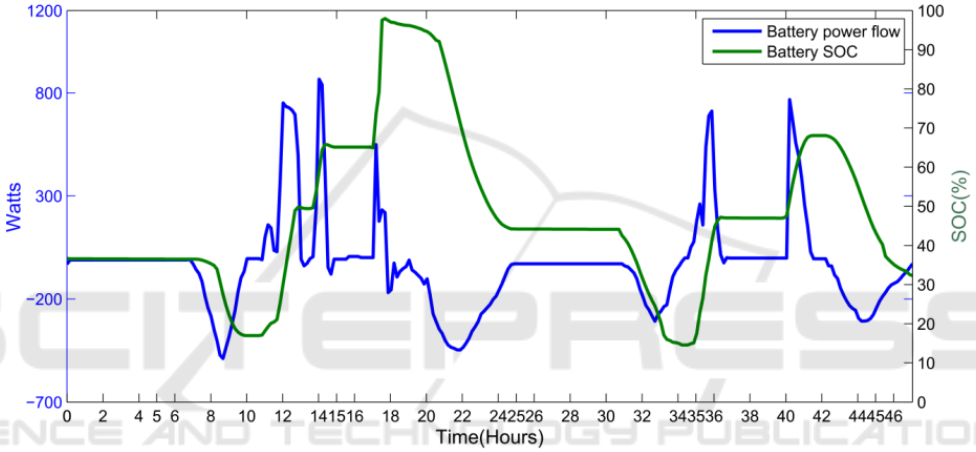

Figure 10: Experiment results for the battery SOC profile.

4 CONCLUSIONS

The experimental results show that the optimal control problem formulated for the peak shaving application of the battery always prioritizes the peaks in the surplus PV and the load demand respectively, as well as maximizing the use of the battery. The problem formulation is consistent for the given size of the system. This allows the prosumer to maximize the use of self-produced electricity and to conduct its own DSM. This way, the prosumer can conduct its own energy management for the benefit of the grid without the need for any external control signals.

Preliminary results with the proposed MPC approach show the ability of the system to deal with the forecast uncertainties. The experiment results also show that the PV power-prediction correction method, together with the moving horizon feature of the MPC, is able to estimate the behavior of PV output power and deal with forecast uncertainties. For the time resolution of 10 minutes (as used in this work), the MPC is not able to take decisions for the deviations that occur within this time interval. So the MPC is still not perfect, and future work is intended to improve its strategy for real-time application. From the experimental results, it was also deduced that with an effective load-prediction model and correction method, the MPC can effectively deal with the load uncertainty as well, which is also part of the future work.

REFERENCES

Castillo-Cagigal, M., Caamano-Martín, E., Matallanas, E., Masa-Bote, D., Gutiérrez, A., Monasterio-Huelin, F., and Jiménez-Leube, J. (2011). PV self-consumption

optimization with storage and active DSM for the residential sector. *Solar Energy*, *85*(9), 2338-2348.

Costanzo, G. T., Kheir, J., and Zhu, G. (2011, June). Peak-load shaving in smart homes via online scheduling. In *Industrial Electronics (ISIE), 2011 IEEE International Symposium on* (pp. 1347-1352). IEEE.

Di Giorgio, A., and Liberati, F. (2014). Near real time load shifting control for residential electricity prosumers under designed and market indexed pricing models. *Applied Energy*, *128*, 119-132.

Arnold, M., and Andersson, G. (2011, August). Model predictive control of energy storage including uncertain forecasts. In *Power Systems Computation Conference (PSCC), Stockholm, Sweden* (Vol. 23, pp. 24-29).

Herter, K. (2007). Residential implementation of critical-peak pricing of electricity. *Energy Policy*, *35*(4), 2121–2130.

Wirth, H., and Schneider, K. (2015). Recent facts about photovoltaics in Germany. *Fraunhofer ISE*, 92.

Morais, H., Faria, P., and Vale, Z. (2014). Demand response design and use based on network locational marginal prices. *International Journal of Electrical Power and Energy Systems*, *61*, 180-191.

Palensky, P., and Dietrich, D. (2011). Demand side management: Demand response, intelligent energy systems, and smart loads. *IEEE transactions on industrial informatics*, *7*(3), 381-388.

Parisio, A., Rikos, E., Tzamalis, G., and Glielmo, L. (2014). Use of model predictive control for experimental microgrid optimization. *Applied Energy*, *115*, 37-46.

Petrollese, M., Valverde, L., Cocco, D., Cau, G., and Guerra, J. (2016). Real-time integration of optimal generation scheduling with MPC for the energy management of a renewable hydrogen-based microgrid. *Applied Energy*, *166*, 96-106.

Riffonneau, Y., Bacha, S., Barruel, F., and Ploix, S. (2011). Optimal power flow management for grid connected PV systems with batteries. *IEEE Transactions on Sustainable Energy*, *2*(3), 309-320.

Schmelas, M., Feldmann, T., da Costa Fernandes, J., and Bollin, E. (2015). Photovoltaics energy prediction under complex conditions for a predictive energy management system. *Journal of Solar Energy Engineering*, *137*(3), 031015.

Spring, A., Becker, G., and Witzmann, R. (2014, June). Grid Voltage Influences Of Reactive Power Flows Of Photovoltaic Inverters With A Power Factor Specification Of One. In *Cired Workshop-Rome* (pp. 11-12)..

Stetz, T., Marten, F., and Braun, M. (2013). Improved low voltage grid-integration of photovoltaic systems in Germany. *IEEE Transactions on Sustainable Energy*, *4*(2), 534-542.

Tonkoski, R., Lopes, L. A. C., and El-Fouly, T. H. M. (2010, July). Droop-based active power curtailment for overvoltage prevention in grid connected PV inverters. In *Industrial Electronics (ISIE), 2010 IEEE International Symposium on* (pp. 2388-2393). IEEE.

Turitsyn, K., Sulc, P., Backhaus, S., and Chertkov, M. (2010, October). Local control of reactive power by distributed photovoltaic generators. In *Smart Grid Communications (SmartGridComm), 2010 First IEEE International Conference on* (pp. 79-84). IEEE.

Weckx, S., Gonzalez, C., and Driesen, J. (2014). Combined central and local active and reactive power control of PV inverters. *IEEE Transactions on Sustainable Energy*, *5*(3), 776-784.

Weniger, J., Bergner, J., and Quaschning, V. (2014). Integration of PV power and load forecasts into the operation of residential PV battery systems. In *4th Solar Integration Workshop* (pp. 383-390).

Wu, Z., Tazvinga, H., and Xia, X. (2015). Demand side management of photovoltaic-battery hybrid system. *Applied Energy*, *148*, 294-304.

Yang, J., Zhang, G., and Ma, K. (2014). Matching supply with demand: A power control and real time pricing approach. *International Journal of Electrical Power and Energy Systems*, *61*, 111-117.